

Histopathological Cancer Detection Using Hybrid Quantum Computing

Reek Majumdar
Civil Engineering Department
Clemson University
Clemson, SC, USA
rmajumd@clemson.edu

Biswaraj Baral
Quantum Computing Group
Qausal AI
San Ramon, CA, USA
biswa@qausal.ai

Bhavika Bhalgamiya
Dept of Physics and Astronomy
Mississippi State University
MS, USA
bgb182@msstate.edu

Taposh Dutta Roy
Quantum Research
SVQCG
San Ramon, CA, USA
taposh.dr@gmail.com

Abstract—We present an effective application of quantum machine learning in the field of healthcare. The study here emphasizes on a classification problem of a histopathological cancer detection using quantum transfer learning. Rather than using single transfer learning model, the work model presented here consists of multiple transfer learning models especially ResNet18, VGG-16, Inception-v3, AlexNet and several variational quantum circuits (VQC) with high expressibility. As a result, we provide a comparative analysis of the models and the best performing transfer learning model with the prediction AUC of ≈ 0.93 for histopathological cancer detection. We also observed that for 1000 images with Resnet18, Hybrid Quantum and Classical (HQC) provided a slightly better accuracy (0.885) than classical (0.88).

Index Terms—Quantum machine learning, Artificial neural network, histopathological cancer detection, quantum transfer learning, variational quantum circuit (VQC).

I. INTRODUCTION

According to American Cancer Society [1] projections for 2023, 1.9 million new cancer cases and 600k deaths are expected to occur in the United States. A recent study shows that 19 to 20 million people die each year due to cancer globally [2]. In such cases, the earliest detection of cancer cells becomes essential to prevent the loss of lives. Artificial intelligence (AI) has a wide range of applications, especially in medicine [3], [4]. As of now, several traditional machine learning methods, including advanced deep learning, self-supervised learning, and transfer learning have been successfully examined and proven to be helpful in detecting different types of cancer including breast cancer [5], [6], burns [7], and histopathological cancers [8].

The work in this study presents an application of hybrid quantum machine learning in medical image processing. It emphasizes on a classification problem of histopathological cancer detection using quantum transfer learning [9]. Rather than using a single learning model, the work model presented here includes multiple transfer learning models, especially ResNet18 [10], VGG-16 [11], Inception v3 [12], AlexNet [13] and different variational quantum circuits (VQC) [14]. As a result, we present an efficient and novel method to develop classification models utilizing hybrid classical and quantum computers in this Noisy Intermediate Scale Quantum (NISQ) system era [15]. We aspire to provide comparable prediction

accuracy and high expressibility utilizing variational quantum circuits.

II. DATA

The dataset used for this work is a set of digital pathology images from the benchmark dataset known as PatchCamelyon(PCam) [8]. This is a large-scale patch-level dataset derived from Camelyon16 [26] data. The aggregate of the patches make up the slide-level image, which can be used to predict likelihood of metastases, stage cancer. Example of patch data samples showing likelihood of cancer is shown in Fig. 1. The data set contains total 100k images. However, we used 10k images in this work model.

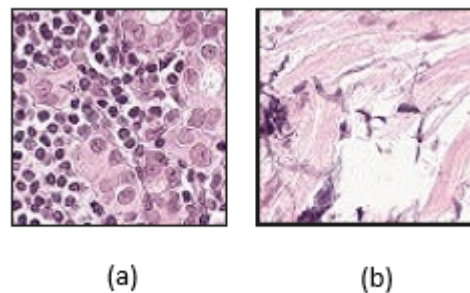


Fig. 1: Data (image) Samples: (a) non-cancerous image (b) cancerous image.

III. METHOD

The framework of the presented work model here consists of four main units. The input unit, classical transfer learning models, VQC-based Quantum Neural Network (QNN), and classical artificial neural network (ANN).

Input unit: The input unit consists of a large data set, up to 100k images. This input data set is divided into train, test, and validation sets. These three sets work as an input for the next unit of the presented work model - transfer learning models, sometimes called multilayer perceptron.

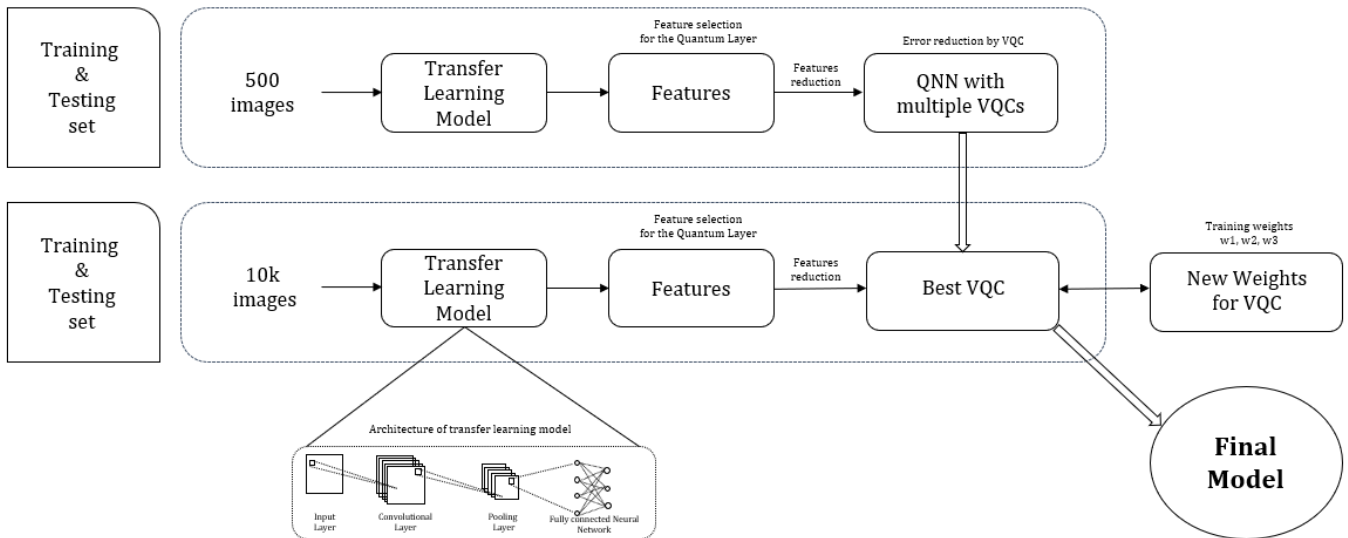


Fig. 2: Framework of the workmodel

Transfer Learning Models: The second unit of this framework is made up of pre-trained transfer learning models [16] trained on the ImageNet data set. Any of the well-known transfer learning models can be utilized in this unit. However, we prefer to analyze ResNet-18, VGG-16, Inception-v3, and AlexNet transfer learning models to start with. Later, we choose the best transfer learning model among these four based on its compatibility with the quantum neural network (QNN) [17] and include that in the final work model. Initially, the original image data is resized and inputted into these transfer learning models. In order to resize images, the new pixel size is chosen based on the input image requirements for the selected transfer learning model. These transfer learning models consist of three layers - a convolutional layer, a pooling layer, and a fully connected layer [18]. The final fully connected layer of these models is modified with a QNN. This QNN is sandwiched between two neuron layers and one output neuron layer based on the number of output classes. The goal of using the transfer learning model as an initial layer in the presented work model is to carefully extract crafted features from images. These features can later be used as a source of input for VQC based QNN [19]. This modified architecture enables us to extend our models to currently available quantum hardware, which cannot handle massive data sets simultaneously.

VQC based QNN: The classical transfer learning models are preceded by VQC based QNN. This unit comprises input and repeated VQC layers. These layers are tested for multiple configurations of single-qubit rotational and two-qubit controlled gates to build the QNN. The features received from the classical CNN

are forwarded and processed by multiple VQCs. After processing features on multiple VQC, we select the best VQC with the highest expressibility. Inherently, VQCs can handle the error caused by the quantum hardware and are used for effective computation on fault-tolerant quantum devices and NISQ devices. As the last step, by performing the quantum measurements, final results from the QNN are obtained.

Classical ANN: The last unit of the presented architecture is a fully connected neural network. The output of the quantum unit (VQC based QNN) is mapped into the final output layer of this unit with softmax activation function [20].

Hyperparameters Tuning: Hyperparameter tuning for improving model performance is one of the important steps of deep learning model. The hyperparameters considered in the presented hybrid model are the number of qubits required to initialize the VQC layer, batch size, learning rate, step size, and optimizers namely Adam and Stochastic Gradient Descent (SGD). For our hybrid models, we have consistently used tanh activation function before inputting the data to VQC layer and softmax function for the final layer of hybrid and classical models. VQC Provides an open way to tune model parameters utilizing variety of activation functions.

The final work model includes the combination of best classical CNN and VQC in order to get an efficient prediction accuracy.

IV. RESULTS

The TABLE I shows the results of the various experiments done on both classical as well as hybrid quantum computing. Column I represents the various classical and hybrid models used in this framework. Number of images used in each model

are shown in column II. Column III provides the percent of accuracy achieved by each transfer learning model. After analysing the performance of each model for various VQC, we selected the best VQC. Column V represents VQC was used (see Fig. 7 in Appendix). Expressibility [28] and number of qubits for VQC in column V are shown in column VI and VII respectively.

Model	Images	Acc	AUC	VQC	Exp	Qbits
Classical CNN	5000	76.10	0.82	N/A	N/A	N/A
Classical CNN2	10000	79.10	0.88	N/A	N/A	N/A
Classical ResNet18	1000	88.00	0.95	N/A	N/A	N/A
Classical ResNet18	10000	89.90	0.96	N/A	N/A	N/A
Hybrid CNN	10000	59.95	N/A	6	0.011	4
Hybrid ResNet18	1000	88.50	0.93	1	1.431	4
Hybrid VGG 16	1000	55.00	0.77	2	1.078	5
Hybrid Inception v3	1000	79.50	N/A	3	1.007	5
Hybrid AlexNet	1000	63.00	0.67	4	0.201	7
Hybrid ResNet18	5000	83.80	0.90	5	0.201	7
Hybrid ResNet18	10000	82.35	0.90	1	1.431	4
HQC ResNet18	10000	84.30	0.90	6	0.011	4

TABLE I: Model Performance and Metric Parameters

We evaluated a total of 12 different major models. For classical transfer learning models, we chose 4 models with varying size of data in quantum transfer learning algorithm explained in [9]. For the hybrid classical and quantum computing models, we evaluated 8 models with different quantum circuits based on VQC, number of qubits [27] in quantum transfer learning algorithm [9].

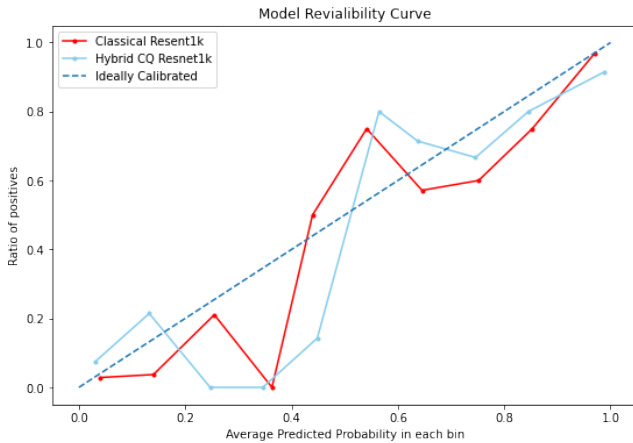


Fig. 3: Reliability curve generated from Classical ResNet18 (solid Red) and Hybrid CQ ResNet18 (solid blue) for total of 1000 images. The ideal reliability curve is shown by dotted blue line for the comparison.

Reliability curve generated from Classical ResNet18 (solid Red) and Hybrid CQ ResNet18 (solid blue) for total of 1000 images is shown in Fig. 3. Model reliability curves [29] [32] provide insights to how the model is calibrated. In case of binary classification [32] [33], model calibration is essential to make sure the model outcomes are not undershooting or overshooting. The central dotted line in Fig. 3 shows a perfectly calibrated model.

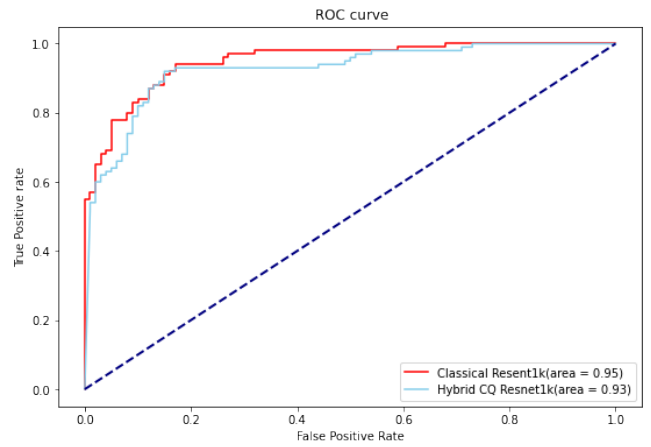


Fig. 4: ROC curve generated from Classical ResNet18 (solid Red) and Hybrid CQ ResNet18 (solid blue). The ideal ROC curve is shown by dotted purple line for the comparison.

ROC curves shown in Fig. 4 shows the False Positive Rate (FPR) vs True Positive Rate (TPR) at different thresholds of classification. It displays the ability of model to distinguish positive class from negative class. Higher area under ROC signifies that the model classifies more positive classes as positive and negative classes as negative. The central dotted line shows that a model have no capability to distinguish positive and negative classes.

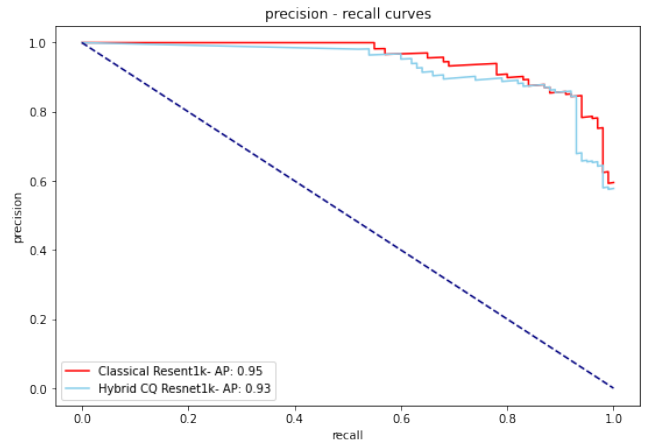


Fig. 5: Precision vs recall curve generated from Classical ResNet18 (solid Red) and Hybrid CQ ResNet18 (solid blue). The ideal Precision - Recall curve is shown by dotted purple line for the comparison.

Fig. 5 shows the precision vs recall plot for different thresholds. Like ROC curve, P-R curve is an important curve to visualize the performance of classification models. The four possible outcomes from binary classification are true positive (TP), false positive (FP), true negative (TN) and false negative (FN). Precision is the ratio of true positives to all the predicted positives and a recall is the ratio of true positives to all the actual positives in the data set.

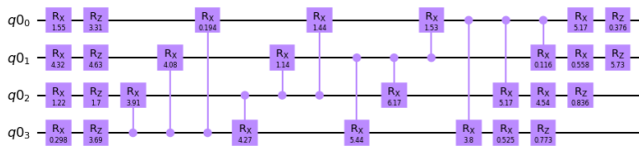


Fig. 6: VQC used in the given model with the highest expressibility with four quantum registers q_0, q_1, q_2, q_3 , and rotational quantum gates.

V. CONCLUSION AND FUTURE WORK

We have tested different combinations of variational quantum circuits in our current work with our chosen transfer learning models (ResNet-18, VGG-16, Inception-V3, and AlexNet). The VQC circuit shown in Figure 4 with the ResNet-18-based transfer learning model provides a performance accuracy of 85 percent, comparable to the performance of the classical ResNet-18 model of 90 percent with similar architecture. It is the first step in exploring the benefits of variational quantum circuits to perform quantum machine-learning tasks for medical image processing.

Currently, we have used the quantum simulators provided by PennyLane [22]. As a next step, we plan to test our trained quantum circuit on actual quantum hardware. We also plan to compare the resiliency of these models against various cyber-attacks, such as adversarial attacks [31]. The distinctive idea presented here was conceived as a result of the quantum system's computing advantages, quantum entanglement's capacity to uncover a variety of counter-intuitive patterns, and the advantages of VQCs in the currently available Noisy-intermediate-scale quantum (NISQ) system. We strongly believe that this frame work can offer reliable machine-learning models for evaluating medical images, and that these models' performance will improve as quantum technology develops along with classical computing.

REFERENCES

- [1] Siegel, RL, Miller, KD, Wagle, NS, Jemal, A, "Cancer statistics, 2023." *Cancer J Clin* 2023; 73(1): 17- 48. doi:10.3322/caac.21763.
- [2] Chhikara, Bhupender S and Parang, Keykavous "Global Cancer Statistics 2022: the trends projection analysis". *Chemical Biology Letters*,10.1 (2023): 451-451.
- [3] Hamamoto, Ryuji, et al "Application of artificial intelligence technology in oncology: Towards the establishment of precision medicine". *Cancers*,12.12 (2020): 3532.
- [4] Yeasmin, Samira. "Benefits of artificial intelligence in medicine". *2019 2nd International Conference on Computer Applications and Information Security (ICCAIS)*, IEEE, 2019.
- [5] Bejnordi, Babak Ehteshami, et al. "Diagnostic assessment of deep learning algorithms for detection of lymph node metastases in women with breast cancer". *Jama*,318.22 (2017): 2199-2210.
- [6] Jin, Xu and Huang, Teng and Wen, Ke and Chi, Mengxian and An, Hong. "HistoSSL: Self-Supervised Representation Learning for Classifying Histopathology Images". *Mathematics*,11.1 (2022): 110.
- [7] Deniz, Erkan and Şengür, Abdulkadir and Kadiroğlu, Zehra and Guo, Yanhui and Bajaj, Varun and Budak, Ümit. "Transfer learning based histopathologic image classification for breast cancer detection". *Health information science and systems*,6 (2018): 1-7.

- [8] Veeling, Bastiaan S., et al. "Rotation equivariant CNNs for digital pathology". *Medical Image Computing and Computer Assisted Intervention-MICCAI 2018: 21st International Conference, Granada, Spain, September 16-20, 2018, Proceedings, Part II 11.* Springer International Publishing, 2018.
- [9] Mari, Andrea, et al. "Transfer learning in hybrid classical-quantum neural networks". *Quantum*, 4 (2020): 340.
- [10] He, Kaiming and Zhang, Xiangyu and Ren, Shaoqing and Sun, Jian, "Deep Residual Learning for Image Recognition" In *Proceedings of the IEEE Conference on Computer Vision and Pattern Recognition*, pages 770-778.IEEE, 2016.
- [11] Simonyan, Karen and Zisserman, Andrew, "Very deep convolutional networks for large-scale image recognition", *International Conference on Learning Representations*, 2014.
- [12] Szegedy, Christian, et al. "Rethinking the inception architecture for computer vision" In *Proceedings of the IEEE Conference on Computer Vision and Pattern Recognition*, pages 2818-2826, 2016.
- [13] Krizhevsky, Alex and Sutskever, Ilya and Hinton, Geoffrey E, "ImageNet classification with deep convolutional neural networks" *Advances in neural information processing systems*, pages 1097-1105, 2012.
- [14] Mitarai, Kosuke, et al. "Quantum circuit learning" *Physical Review A*, 98.3 (2018): 032309.
- [15] Preskill, John. "Quantum computing in the NISQ era and beyond", *Verein zur Förderung des Open Access Publizierens in den Quantenwissenschaften*
- [16] Niu, Shuteng, et al. "A decade survey of transfer learning (2010-2020)", *IEEE Transactions on Artificial Intelligence*, 1.2 (2020): 151-166..
- [17] Schuld, Maria and Sinayskiy, Ilya and Petruccione, Francesco, "The quest for a quantum neural network". *Quantum Information Processing*, Springer, pages 2567-2586, 2014.
- [18] Gu, Jiuxiang, et al. "Pattern recognition", In *Elsevier*, 2018.
- [19] Qi, Jun, et al. "Theoretical error performance analysis for variational quantum circuit based functional regression". *Nature Publishing Group UK London*, 2023.
- [20] Goodfellow, Ian and Bengio, Yoshua and Courville, Aaron, "Deep learning". MIT press, 2016.
- [21] Sim, Sukin, Peter D. Johnson, and Alán Aspuru-Guzik, "Expressibility and entangling capability of parameterized quantum circuits for hybrid quantum-classical algorithms." *Advanced Quantum Technologies* 2.12 (2019): 1900070.
- [22] Bergholm, Ville, et al. "PennyLane: Automatic differentiation of hybrid quantum-classical computations." *arXiv preprint arXiv:1811.04968* (2018).
- [23] Wang, Yazhen and Liu, Hongzhi, "Quantum Computing in a Statistical Context" *Annual Review of Statistics and Its Application* volume 9, pages 479-504, (2022).
- [24] Biamonte, Jacob, et al., "Quantum machine learning." *Nature* 549.7671, pages 195-202, (2017).
- [25] Pirhooshayan, Mohammad, and Tamas Terlaky., "Quantum circuit design search." *Quantum Machine Intelligence* 3 pages 1-14, (2021).
- [26] Babak Ehteshami Bejnordi., et al., "Diagnostic assessment of deep learning algorithms for detection of lymph node metastases in women with breast cancer." *JAMA* 318(22) pages 2199-2210, (2017).
- [27] Schumacher, Benjamin, "Quantum coding." *Physical Review A* 51.4 (1995): 2738.
- [28] Yano, Hiroshi, et al., "Efficient discrete feature encoding for variational quantum classifier." *2020 IEEE International Conference on Quantum Computing and Engineering (QCE)* IEEE, 2020.
- [29] Steyerberg, Ewout Willem et al., "Performance measures for prediction models and markers: evaluation of predictions and classifications" *2020 Revista espanola de cardiologia* 64 9 (2011): 788-94.
- [30] Qi, Jun, Chao-Han Huck Yang, and Pin-Yu Chen., "Qtn-vqc: An end-to-end learning framework for quantum neural networks." *arXiv preprint arXiv:2110.03861* (2021)
- [31] Madry, Aleksander, et al., "Towards deep learning models resistant to adversarial attacks." *arXiv preprint arXiv:1706.06083* (2017)
- [32] Lucena, Brian., "Spline-based probability calibration." *arXiv preprint arXiv:1809.07751* (2018)
- [33] Smola, Alexander J, "Probabilities for sv machines." *Advances in Large Margin Classifiers, MIT Press* (2000): 61-73.

APPENDIX

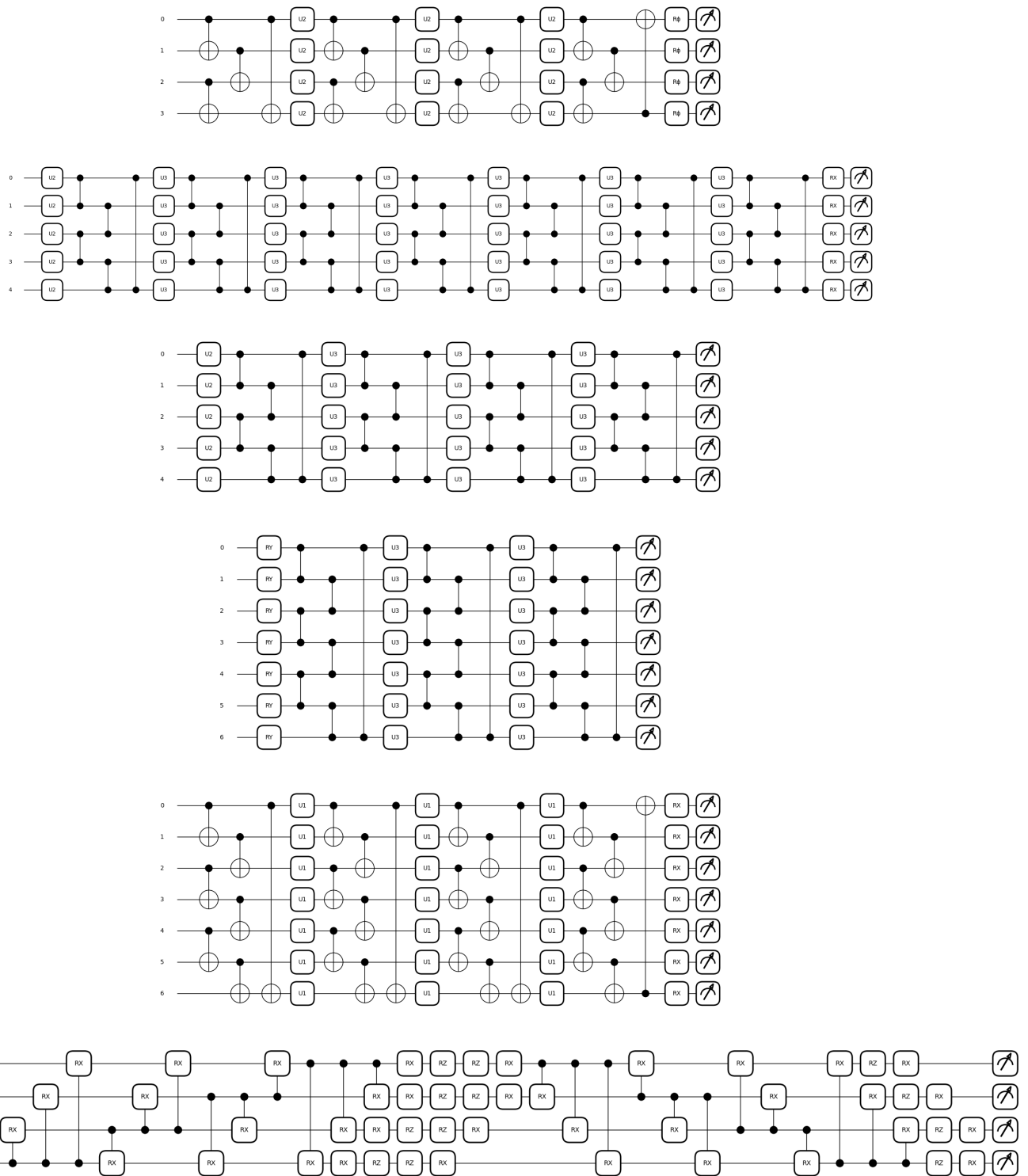


Fig. 7: Appendix A1. Figures show the 21 (starting from top of the page) -26 (bottom of the page) different variational quantum circuits that were generated as part of our analysis. We evaluated all these circuits using the pennylane quantum simulator and selected the better performing ones using the circuits expressibility scores.

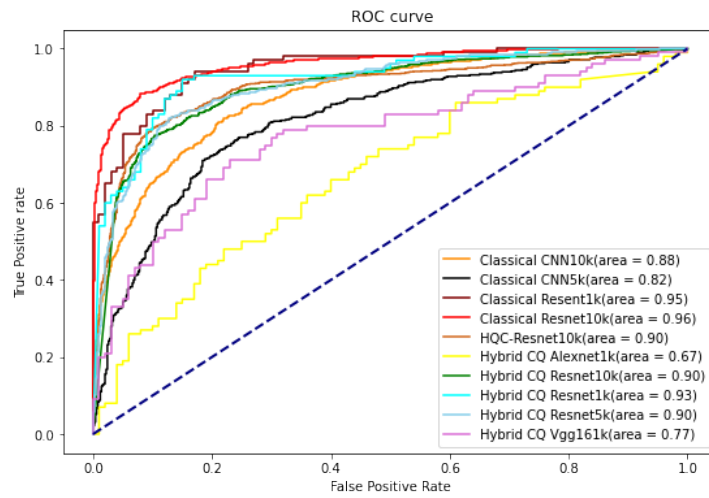


Fig. 8: Appendix A2. ROC curves obtained from different models

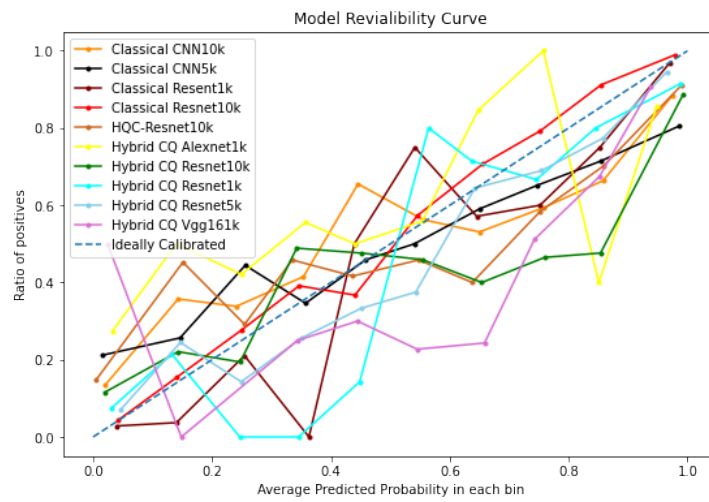


Fig. 9: Appendix A3. Reliability curves obtained from different models

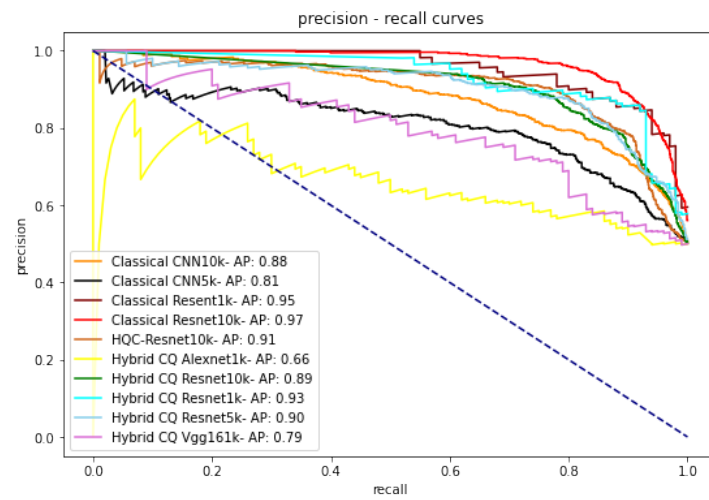


Fig. 10: Appendix A4. PR curves obtained from different models